

Separation of propagating and non-propagating components in surface EMG

Original

Separation of propagating and non-propagating components in surface EMG / Mesin, Luca; Kandoor, A. K. R.; Merletti, Roberto. - In: BIOMEDICAL SIGNAL PROCESSING AND CONTROL. - ISSN 1746-8094. - STAMPA. - 3:(2008), pp. 126-137. [10.1016/j.bspc.2007.11.002]

Availability:

This version is available at: 11583/1913140 since: 2017-07-21T14:51:25Z

Publisher:

Elsevier

Published

DOI:10.1016/j.bspc.2007.11.002

Terms of use:

This article is made available under terms and conditions as specified in the corresponding bibliographic description in the repository

Publisher copyright

Elsevier postprint/Author's Accepted Manuscript

© 2008. This manuscript version is made available under the CC-BY-NC-ND 4.0 license
<http://creativecommons.org/licenses/by-nc-nd/4.0/>. The final authenticated version is available online at:
<http://dx.doi.org/10.1016/j.bspc.2007.11.002>

(Article begins on next page)

Separation of propagating and non propagating components in surface EMG

Luca Mesin¹, Arun Kumar Reddy Kandoor², Roberto Merletti¹

*¹Laboratorio di Ingegneria del Sistema Neuromuscolare (LISiN), Dipartimento di
Elettronica, Politecnico di Torino, Torino, Italy.*

*²Department of Electronics and Communication Engineering,
Indian Institute of Technology, Guwahati, India.*

Keywords: conduction velocity, linear electrode arrays, adaptive filters, surface EMG.

Running title: identification of non propagating components in EMG signals

Address for correspondence:

Luca Mesin, Ph.D.

Dipartimento di Elettronica, Politecnico di Torino; Corso Duca degli Abruzzi 24, Torino, 10129 ITALY

Tel. 0039-011-4330476; Fax. 0039-0114330404;

e-mail: luca.mesin@polito.it

Acknowledgements. This work was supported by grants from the European Space Agency (contract C15097/01/NL/SH) and from Compagnia di San Paolo and Fondazione CRT, Torino, Italy. The work in [13], providing a basis for this contribution, was done at the NeuroMuscular Research Center of Boston University.

ABSTRACT

Surface electromyogram (EMG) detected by electrode arrays along the muscle fibre direction can be approximated by the sum of propagating and non propagating components. A technique to separate propagating and non propagating components in surface EMG signals is developed. The first step is an adaptive filter, which allows obtaining an estimation of the delay between signals detected at different channels and a first estimate of propagating and non-propagating components; the second step is used to optimise the estimation of the two components. The method is applicable to signals with one propagating and one non propagating component. It was optimised on simulated signals, and then applied to single motor unit action potentials (MUAP) and to M-waves.

The new method was first tested on phenomenological signals constituted by the sum of a propagating and a non propagating signal and then applied to simulated and experimental EMG signals. Simulated signals were generated by a cylindrical, layered volume conductor model. Experimental signals were monopolar surface EMG signals collected from the abductor pollicis brevis muscle and M-waves recorded during transcutaneous electrical stimulation of the biceps muscle. The technique may find different applications: in single motor unit (MU) studies, a) for decreasing the variability and bias of CV estimates due to the presence of the non propagating components, b) for estimating automatically the length of the muscle fibres from only three detected channels and c) for removal of the stimulation artifact from electrically elicited EMG (M-wave).

1. INTRODUCTION

Surface electromyogram (EMG) signals detected by electrode arrays along the direction of the muscle fibres can be approximated by the sum of propagating and non propagating components [1]. Propagating components are associated to the propagating of the transmembrane current along the muscle fibres. The non propagating component in surface EMG signals is mainly due to the generation of the transmembrane currents at the neuromuscular junctions and to their extinction at the tendon endings (end of fibre effect) [2][3]. The generation and the extinction of the transmembrane current are associated to far field potentials simultaneously recorded by all the electrodes of the

detection array. Crosstalk from other muscles may contribute in introducing non propagating components in the EMG signals, as generation and extinction effects give the main contribution to crosstalk. For electrically elicited contractions, an important non propagating signal is the stimulation artifact.

The presence of non propagating components affects the estimation of EMG parameters. For example, the non propagating component due to the end of fibre effect contributes to the high frequency portion of the spectrum of the EMG signal. In the case of dynamic contractions the tendons move with respect to the detection system, and, as a consequence, the end of fibre effect changes in amplitude and duration. The effect of muscle shortening on parameters extracted from the EMG signal spectrum was addressed in previous papers [4][5].

Muscle fibre conduction velocity (CV) is another variable whose estimates are strongly affected by non propagating components. It reflects important properties of the membrane of the muscle fibres and is thus indicative of the peripheral condition of the neuromuscular system. CV can be estimated from surface EMG electrode arrays located between the innervation zone and the tendon region along the direction of the muscle fibres [6][7], by evaluating the delay of propagation of the signals [8]. As the signals detected from different channels are not simply constituted by a propagating wave, there is not a unique mathematical definition of the delay between detected potentials, but many definitions are possible [3] (associated to different estimation methods, e.g. methods based on maximum likelihood, reference points, detection of spectral dips, etc.). Different methods for CV estimation have different sensitivities to non propagating signal components. The effect of these components depends on the spatial filters applied for signal detection [9][10]. Specific combinations of spatial filters and estimation methods may be better than others in reducing the bias in CV estimates due to non propagating signals. Double differentiation of the detected signals, for example, usually improves the estimate of CV [1].

A recent approach for CV estimation is based on the application of a pair of spatial filters and on the estimation of the temporal filters (related to the spatial filters by the CV to be estimated) that best align the signals and compensate for the effect of the applied spatial filters [11]. On the basis of such

idea, a method has been recently developed [12] for the identification of the non propagating components. The method provides the optimal choice of a pair of spatial filters which reduce the effect of non propagating components in the delay estimation. However, if the non propagating components have about the same amplitude in all the detected channels, all filter pairs can eliminate them, and all filters give a good CV estimate, but non propagating components cannot be estimated.

The method proposed in this work is focused on the separation of non propagating and propagating components from the compound signal and is based on two steps. The first is an improvement of an adaptive filter technique proposed in [13]. It provides a means to estimate the delay between signals detected at different channels and a first estimate of the propagating and non-propagating components. The second step is used to optimise the estimation of such components.

In the case of electrically elicited signals (M-waves), the main non propagating component is given by the stimulation artifact (see [14] for a characterisation of artifact). The identification of artifact on M-waves was addressed in many papers [14]. The removal of the stimulation artifact is important to extract information from the M-waves, mainly when the artifact is partially superimposed on the M-waves. Recent results were obtained using a neural network [15].

The method proposed in this paper was applied both to simulated and experimental signals, to identify the non propagating components due both to the generation/extinction effects and to the stimulation artifact (for electrically elicited EMG signals). Furthermore, when applied to monopolar simulated single fibre action potentials (SFAP), the method allows the estimation of the fibre semi-length (length from the innervation zone to the tendon closer to the detection array).

2. METHODS

A. Signal model and notations

In order to obtain a simple model of surface electromyogram (EMG), we considered a portion of a muscle with parallel and finite fibres. Under such hypothesis, the motor unit action potentials (MUAP) detected over the skin surface propagate without change of shape from the MU innervation zone to the tendon endings. In these ideal conditions, the EMG signals detected by an array along the fibre direction can be approximated as a linear combination of propagating and non-propagating

components. The non-propagating signals are due to generation and extinction effects in voluntary contractions, and also due to stimulation artifact in electrically elicited contractions.

Some of the factors perturbing these ideal conditions are the misalignment of the detection array with respect to the fibre direction, the inclination of the fibres with respect to the detection surface, the presence of tissue in-homogeneities. Such factors affect the detected potentials introducing amplitude variations and shape perturbations in the signals with respect to the ideal case.

Only amplitude variations across channels are considered in this method. The method is based on the analysis of three surface EMG signals, but could be extended to more. Consider:

$$\begin{aligned} E_0(t) &= V_0(t) + V_1(t) \\ E_1(t) &= a_{10}V_0(t) + a_{11}V_1(t - \tau) \\ E_2(t) &= a_{20}V_0(t) + a_{21}V_1(t - 2\tau) \end{aligned} \quad (1)$$

where $E_i(t)$ ($i = 0,1,2$) are the recorded signals, $V_0(t)$ is the non propagating component, $V_1(t)$ is the propagating component, and the coefficients a_{ij} ($i=1,2; j=0,1$) are the unknown elements of the

matrix $\underline{\underline{A}} = \begin{bmatrix} 1 & 1 \\ a_{10} & a_{11} \\ a_{20} & a_{21} \end{bmatrix}$, relating the measures $\underline{\underline{E}}(t) = \begin{bmatrix} E_0(t) \\ E_1(t) \\ E_2(t) \end{bmatrix}$ to the unknown components $\underline{\underline{V}}(t) = \begin{bmatrix} V_0(t) \\ V_1(t) \end{bmatrix}$. In

general, considering detection channels located away from the innervation zone and from the tendons, for inter-channel distance of the order of 2.5 to 10 mm all the weighting coefficients a_{ij} are close to unity. We constrained the unknown coefficients a_{ij} to be between 0.5 and 1.5.

The assumptions of model (1) are the following: 1) both the propagating and the non propagating components maintain the same shape in the three recorded channels and each is multiplied by an unknown coefficient; 2) the delay between propagating components detected in adjacent channels is constant.

In model (1), the only available data are the recorded signals $E_i(t)$. The delay τ , the shape of the propagating and non propagating components and their amplitudes in the three channels are unknown and should be estimated without any a-priori information.

The problem will be first solved by applying an adaptive filter, obtaining a first approximated solution. Such a solution will then be optimised.

B. Adaptive filtering method

An improvement of the adaptive filter proposed in [13] is the first step to the solution of the problem. We proceed in Fourier domain instead of z-domain as proposed in [13] for easier computations. In Section B.1 the method proposed in [13] is briefly described. In Section B.2 the method is improved.

B.1 Algorithm for adaptive filter method

Let us suppose that the delay τ is known. Taking the Fourier transform of system (1) and rearranging the equations, one can write them in matrix form as shown below

$$\underline{\underline{\tilde{A}}}\hat{\underline{V}} = \begin{bmatrix} I & I & \hat{E}_0(\omega) \\ a_{10} & a_{11}e^{-j\omega\tau} & \hat{E}_1(\omega) \\ a_{20} & a_{21}e^{-j\omega 2\tau} & \hat{E}_2(\omega) \end{bmatrix} \begin{bmatrix} \hat{V}_0(\omega) \\ \hat{V}_1(\omega) \\ -I \end{bmatrix} = 0 \quad (2)$$

where ω is the angular frequency and the symbol $(\hat{\cdot})$ indicates Fourier transformation. The above equations will be satisfied when the determinant of the 3x3 matrix $\underline{\underline{\tilde{A}}}$ is identically zero, which means

$$a_{11}e^{j\omega\tau}\hat{E}_2(\omega) + a_{10}a_{21}e^{j\omega 2\tau}\hat{E}_0(\omega) + a_{20}\hat{E}_1(\omega) - a_{11}a_{20}e^{j\omega\tau}\hat{E}_0(\omega) - a_{21}e^{j\omega 2\tau}\hat{E}_1(\omega) - a_{10}\hat{E}_2(\omega) = 0. \quad (3)$$

Eq. (3) can be rewritten in the following form (useful for the implementation of an iterative search of the solution)

$$\hat{E}_2(\omega) = w_{01}e^{j\omega\tau}\hat{E}_0(\omega) + w_{02}e^{j\omega 2\tau}\hat{E}_0(\omega) + w_{10}\hat{E}_1(\omega) + w_{12}e^{j\omega 2\tau}\hat{E}_1(\omega) + w_{21}e^{j\omega\tau}\hat{E}_2(\omega) \quad (4)$$

where $w_{01} = -\frac{a_{11}a_{20}}{a_{10}}$, $w_{02} = a_{21}$, $w_{10} = \frac{a_{20}}{a_{10}}$, $w_{12} = -\frac{a_{21}}{a_{10}}$, $w_{21} = \frac{a_{11}}{a_{10}}$. The weights w_{ij} are not known

a-priori. Thus, for an arbitrary choice of the weights w_{ij} , the right hand side of Eq. (4) can be considered only as an approximation of $\hat{E}_2(\omega)$.

Two approaches can be used to estimate the unknown weights w_{ij} , depending on whether or not on-line processing is required: 1. Linear parameter estimation (Off-line); 2. Adaptive LMS algorithm (On-line). Both approaches provide the same result (see [16] for details).

The first method was used. Eq. (4) can be written in matrix form as follows

$$\overline{\hat{E}_2} = \overline{\underline{E}} \overline{\underline{W}} \quad (5)$$

where: $\overline{W} = [w_{01} \ w_{02} \ w_{10} \ w_{12} \ w_{21}]^T$, $\overline{E} = \mathfrak{F}[E_0(t-\tau) \ E_0(t-2\tau) \ E_1(t) \ E_1(t-2\tau) \ E_2(t-\tau)]$,

where \mathfrak{F} indicates Fourier transform. The above system is linear in the unknown vector \overline{W} . Its optimal solution in the least mean squares (LMS) sense is calculated by taking the Moore-Penrose pseudo-inverse of \overline{E}

$$\Rightarrow \overline{W}^* = \overline{E}^{\#} \overline{E}_2 \quad (6)$$

the symbol * indicating LMS-optimal, and # denoting pseudo-inverse.

Once the weights w_{ij} are obtained, the unknown coefficients of the matrix \underline{A} can be obtained by inverting the definitions of the weights w_{ij} in terms of the elements a_{ij} of the matrix \underline{A} , written in the following matrix form

$$\underline{W}\underline{a} = \underline{w}_0 \Rightarrow \begin{bmatrix} 0 & 1 & 0 & 0 \\ 0 & 0 & 0 & 1 \\ w_{10} & 0 & -1 & 0 \\ w_{12} & 0 & 0 & 1 \\ w_{21} & -1 & 0 & 0 \end{bmatrix} \cdot \begin{bmatrix} a_{10} \\ a_{11} \\ a_{20} \\ a_{21} \end{bmatrix} = \begin{bmatrix} -w_{10} w_{01} \\ w_{02} \\ 0 \\ 0 \\ 0 \end{bmatrix} \quad (7)$$

From Eq. (7), the unknown elements a_{ij} of the matrix \underline{A} (contained in Eq. (7) in the vector \underline{a}) are computed optimally in the LMS sense by pseudo-inverting the matrix \underline{W} .

Once the coefficient matrix \underline{A} is obtained as explained above, the propagating and non-propagating components are estimated by pseudo-inverting the matrix \underline{A} and applying it to the data (i.e., pseudo-inverting Eq. (2)).

B.2 Limitations of the adaptive filter algorithm

The adaptive filter method, as introduced in [13], has two main limitations. 1) The method requires an a-priori knowledge of the delay τ . 2) The method is sensitive to very small shape and delay perturbations of the propagating components and the performance worsens in presence of additive noise.

A new version of the algorithm was developed to estimate the delay τ by minimising the reconstruction error (defined as the RMS error between the three measured signals and those

reconstructed by summing the estimated propagating and non propagating components) with respect to τ (with no limits in resolution, implementing the minimisation process in the frequency domain). The algorithm was implemented with the software *Matlab* (version 7.0), using the function *fminbnd*. The minimum was searched for values of delays related to physiological values of CV (between 2 and 8 m/s).

To reduce the sensitivity to noise and shape perturbations, the optimisation method was implemented, as described in the following section.

The algorithm is described in Figure 1.

Figures 1 about here

C. Optimisation method for estimating propagating and non propagating components

Using the modified adaptive filter approach we estimated 1) the delay between propagating components, 2) the weight matrix $\underline{\underline{A}}$, 3) the two unknown functions $\underline{\underline{V}}(t)$ (propagating and non-propagating components). With this approach, the estimated non-propagating components are not well localised in time (see Results). When the locations of the innervation zone and tendons are of interest (for example, to estimate fibre semi-length), this limitation is not acceptable. As a consequence of the error in the estimation of the non-propagating component, also the estimation of the propagating signal presents problems.

In order to improve the estimated propagating and non-propagating components, an optimisation process is proposed in this work. The optimisation is based on the minimisation of an error function.

The error function was chosen as the linear combination of two terms:

1. the RMS error between the data and their reconstruction $RMS = \left\| \underline{\underline{E}}(t) - \underline{\underline{A}}\underline{\underline{V}}(t) \right\|_2^2$;
2. the energy of the non propagating component.

The resulting error function is the following

$$EF = \left\| \underline{\underline{E}}(t) - \hat{\underline{\underline{A}}}\underline{\underline{V}}(t; \hat{\underline{\underline{A}}}) \right\|_2^2 + \gamma \left\| V_0(t; \hat{\underline{\underline{A}}}) \right\|_2^2 \quad (8)$$

where γ is a non negative parameter, referred to as regularisation parameter (whose choice is explained in the next paragraph). For a fixed matrix $\underline{\underline{A}}$, the unknown functions \underline{V} are chosen as those minimising the RMS error in the reconstruction of the $\underline{E}(t)$ signals

$$\underline{V}(t) = \min_{\underline{x}} \left\| \underline{E}(t) - \underline{\underline{A}}\underline{x}(t) \right\|_2^2 \quad \Rightarrow \quad \underline{V}(t) = \underline{\underline{A}}^{\#} \underline{E}(t) \quad (9)$$

the symbol # indicating the Moore-Penrose pseudo inverse of a rectangular matrix. Substituting the expression of the unknown functions \underline{V} from Eq. (9), the error function EF defined in Eq. (8) is only a function of the unknown matrix $\underline{\underline{A}}$. Thus, the minimisation problem can be written as

$$\underline{\underline{A}}^{opt} = \min_{\underline{\underline{A}}} \left\| \underline{E}(t) - \hat{\underline{\underline{A}}}\underline{V}(t; \underline{\underline{A}}) \right\|_2^2 + \gamma \left\| \underline{V}_0(t; \underline{\underline{A}}) \right\|^2 \quad \text{where} \quad \underline{V}(t; \underline{\underline{A}}) = \underline{\underline{A}}^{\#} \underline{E}(t) \quad (10)$$

The elements of the unknown matrix $\underline{\underline{A}}^{opt}$ were constrained to be in the range [0.5; 1.5] (refer to Section 2.A). The Matlab function *fmincon* was used for this constrained optimisation process. The coefficient matrix and the time delay estimated after applying the adaptive filter method are used as the starting point for the optimisation process to obtain the matrix $\underline{\underline{A}}^{opt}$ that satisfies (10). The correspondent vector of functions \underline{V} , also defined in (10), provides the estimated propagating and non propagating components.

The choice of the regularisation parameter γ should consider the trade-off between the degree of regularity of the solution and its fit to the data, reflecting an *approximation error* and a *data noise error* [17]. We propose a technique to choose the penalisation parameter which was fit on the simulated signals. With very low values for γ , the RMS error in the reconstruction and the energy of the non propagating component $V_0(t)$ (i.e., the regularisation function) is close to that obtained by the adaptive filter method. Increasing γ , the norm of the estimated non propagating component assumes a greater importance in the error function EF. As a consequence, the minimisation of the error function EF determines the increase of the RMS error in reconstructing the original signals $\underline{E}(t)$ and the decreasing of the energy of the non propagating component for increasing values of γ . At a certain value of γ , there's an abrupt change of both RMS and energy of $V_0(t)$, giving a sigmoid

like shape of the RMS error and energy of $V_0(t)$ as a function of the regularisation parameter γ . Such a value of γ , referred to as γ^{opt} , can be detected automatically, since it corresponds to the maximum of the absolute value of the derivative of the RMS error and of the energy of the estimated non propagating component $V_0(t)$ as a function of γ . It was empirically verified in simulations that the solution corresponding to γ^{opt} gives an optimal reconstruction of the propagating and non-propagating components (see the example in Figure 3a, 3b). This value of γ was then chosen in the definition of the error function EF defined in (8).

Figures 2, 3 about here

D. Estimation of fibre semi-length from the detected generation and extinction effects

The non propagating components in a single MUAP are constituted by the generation and the extinction effects. When monopolar signals are considered, such effects are quite large and both of them can be estimated by the method (see the Result section). The fibre semi-length L (the length of the fibre from the innervation zone to the tendon closer to the detection array) was estimated from the estimated CV and the estimated time delay $\Delta\tau$ between the generation and the extinction effects:

$$L = CV \cdot \Delta\tau \quad (11)$$

The time delay between the generation and the extinction effects $\Delta\tau$ was estimated by the following steps.

1. Identification of the supports of the generation and extinction effects.
2. Separation of the two effects, by considering the non propagating component on the support of the generation and of the extinction effects respectively, as determined at step 1.
3. Estimation of the mean values τ_g, τ_e of the generation/extinction effects (centroid of the non propagating component evaluated in the support of the generation/extinction effects, respectively).
4. $\Delta\tau = \tau_e - \tau_g$.

The time supports of the generation and extinction effects were obtained by selecting the time samples for which the non propagating component was larger than a threshold (chosen as the 10% of

the maximum value of the non propagating component). Two separated time interval are obtained, automatically identified and assigned to the generation and extinction effects.

E. Signals considered for the validation of the method

To optimise the method and to give a quantitative validation of its performances, phenomenological and simulated signals were considered. Experimental signals were finally considered as examples of application of the method.

E1. Phenomenological signals

As phenomenological signals we indicate three signals obtained as sum of propagating and non propagating components with a simple analytical expression. The propagating signal was described

by the second derivative of a Gaussian function $v_p(t) = \frac{d^2}{dt^2} e^{-\frac{(t-\mu_p)^2}{2\sigma_p^2}}$, resembling the propagating

component in a monopolar EMG signal. The non propagating component was modelled as a Gaussian

function: $v_{np}(t) = e^{-\frac{(t-\mu_{np})^2}{2\sigma_{np}^2}}$. Phenomenological signals are useful to validate the method as all the

parameters of the model (coefficients matrix, propagating and non propagating components) are

known. As done in [12], we used such signals to assess the effect of perturbations of the initial

hypotheses on the performances of the method. The perturbations introduced were in the delay and in

the width of the propagating components. Delay perturbation was assessed imposing for the second

channel a delay of propagating component slightly different than τ : $\tau_p = \frac{100+p}{100}\tau$, where τ_p is the

perturbed delay of the propagating component and p is the amount of the change (in % of τ).

Width changes were included in the propagating σ_p component by changing the variance σ_p :

$\sigma_p^p = \frac{100+p}{100}\sigma_p$, where σ_p^p is the perturbed width of the propagating component and p is the amount

of the change (in % of σ_p).

A white noise with 20 dB of signal to noise ratio (SNR) was added to the phenomenological signals.

E2. Simulation of single fibre action potentials

A cylindrical layer model [18] (four layers: bone, 20 mm radius, conductivity 0.02 S/m; muscle, thickness 26 mm, longitudinal conductivity 0.5 S/m, transversal conductivity 0.1 S/m; fat, thickness 3 mm, conductivity 0.05 S/m; skin, thickness 1 mm, conductivity 0.5 S/m) was used to simulate SFAP related to fibres with different depth and length, and with different transversal distance and inclination with respect to the detection array of three monopolar channels (point electrodes with 5 mm inter-electrode distance). A white noise with 20 dB SNR was added.

For simulated SFAP, as the CV and the positions of the innervation zone and tendons were known, it was possible to identify the support of the generation and of the end of fibre effects. By interpolation, the propagating component was estimated for each simulated signal without additive noise (see Figure 2). Three propagating components were estimated, one for each channel. The three estimated propagating components have been aligned and averaged to improve the estimate. The non propagating components of the three channels were then estimated by subtracting the estimate of the propagating component (properly delayed) from the input signals.

It is worth noticing that the interpolation method described in Figure 2 is available only for simulated signals for which the temporal supports of the generation and extinction phenomena are known.

Figures 4 and 5 about here

E3. Experimental signals

Both single motor unit (MU) voluntary contractions and elicited contractions were considered, as described in a) and b).

a) The surface EMG signals related to voluntary contraction were collected from the abductor pollicis brevis muscle by a linear array of 3 electrodes (inter-electrode distance 5 mm, electrodes 1 mm diameter), located between the most distal tendon and the muscle belly, along the direction of the muscle fibres; the reference electrode was placed at the wrist; they were amplified (EMG amplifier, EMG-16, LISiN – Ottino Bioengineering, bandwidth 10-500 Hz), sampled at 2048 Hz, and stored after a 12 bit A/D conversion. The subject was asked to perform a contraction 60 s long, at a low

force level, in order to activate a few MUs. The signals were decomposed to identify single MUAPs with the decomposition method introduced in [19], and spike-triggered averaged [20].

b) Electrically elicited surface EMG signals were recorded during transcutaneous electrical stimulation of the biceps brachii muscle. The same EMG amplifier as before was used to record three single differential signals. The stimulation was provided by a programmable neuromuscular stimulator with a hybrid output stage. The EMG signals were detected with a linear array, in single differential configuration, with 5 mm inter-electrode and inter-channel distance.

3. RESULTS

The adaptive filter and optimised methods were applied to phenomenological and simulated signals, in order to compare their performances. They were then applied to experimental signals, to give representative examples of application.

A. Stability of the method on delay and shape perturbation of the propagating component

Figure 4 shows the performance of the optimised method compared to the adaptive filter technique when shape and delay perturbations are applied to the propagating components (phenomenological signals described in Section 2.E1). The input signals (without additive noise), the correct components and their reconstruction with the adaptive filter technique and the optimised method are shown, both in the case of shape perturbation a) and delay perturbation b) of the propagating component. After optimisation, localisation of the non-propagating component improved.

Figures 4 c) and d) show the performance of the proposed method for varying level of perturbations in the phenomenological signals compared to the adaptive filter algorithm (no noise added). To quantify the correctness of the reconstruction, the following RMS errors were studied: 1) the RMS error between the estimated propagating component and the simulated one (without perturbation); 2) the RMS error between the estimated non-propagating component and the simulated one. Both the results obtained by the method of adaptive filter and the optimised method are shown. In general, the optimisation method improved the estimation.

B. Application to simulated signals

An example of application of the adaptive filter method and of the optimised method to simulated signals (described in Section 2.E2) is shown in Figure 5. The simulated signals are shown in a). Figure 5 b) and 5 c) show the non propagating components as obtained by interpolation (i.e., approximately the real non propagating components) and by adaptive filter before and after optimisation, respectively. The non propagating components identified by the two methods are also shown in d). Both generation and end of fibre components are identified. After optimisation, localisation of the non-propagating component improved. Figure 5 e) and 5 f) show the propagating component estimated by adaptive filter and optimisation method, respectively.

In Figure 6 the following simulations related to different anatomies were considered: a) variation of depth of the fibre within the muscle; b) variation of semi-length of the fibre; c) variation of transversal distance with respect to the detection array; d) variation of the angle of inclination of the fibre with respect to the detection array. To quantify the correctness of the reconstruction, the following RMS errors were studied: 1) the RMS error between the propagating component estimated by the separation method and the propagating component estimated by interpolation on the simulated signals; 2) the RMS error between the non-propagating component estimated by the separation method and the non-propagating component estimated by interpolation on the simulated signals. Both the results obtained by the method of adaptive filter and the optimised method are shown. In general the percentage error increases for increased depth within the muscle, for shorter fibres and for fibres with large transversal distance with respect to the detection system; in such cases the weight of non propagating components increased. The percentage error changes slightly by varying the angle between the fibre and the detection array: we should note that with a positive angle between the fibre and the detection array the hypothesis that the propagating components in different channels have respectively the same shape on all channels is no longer true. In general, the optimisation method improved the estimation.

Figure 7 shows the application of the adaptive filter and optimised method to the estimation of fibre semi-length. In a), the method to estimate fibre length is explained. The two methods were applied to estimate fibre semi-length for different lengths of the simulated fibres. In b), c), d) the percentage estimation error (percentage error with respect to the actual fibre semi-length) relative to superficial

fibres under the array (3 mm depth), deeper fibres (6 mm deep) and superficial fibres at a lateral distance (5 mm transversal distance and 3 mm depth) are shown. Since by increasing depth and transversal distance the weights of the generation and extinction effects in the signals increase, the estimation improves.

Figures 6 and 7 about here

C. Experimental data

The results of processing some experimental data are shown in Figure 8. In a), b), c) an example of application to an array of three monopolar surface MUAP signals from abductor pollicis muscle during a voluntary contraction is considered. Before applying the method described in Section 2, each monopolar signal was normalised with respect to its negative peak value in order to reduce the variations in the amplitude of the propagating component across the channels. After the application of the method, the results were de-normalised.

Figure 8 d), e), f) show the results in removing the stimulation artifact generated in the recorded surface EMG signal during transcutaneous electrical stimulation of the biceps brachii muscle. The artifact is considered as the non propagating component to be identified. Both the adaptive filter and the proposed optimisation succeed in identifying the artifact. The optimisation method improves localisation with respect to adaptive filter as the amplitude of the estimated non propagating component superimposed to the propagating M-wave (probably due to shape perturbations of the propagating wave) is lower. We expect that the estimation of the M-wave (i.e., the propagating component) is improved by using the optimised method.

Figures 8 about here

4. DISCUSSION

This study proposes a new method for the identification of propagating and non-propagating components from an array providing three adjacent channels of surface EMG. It is based on an adaptive filter technique, which estimates the delay between the propagating signals and provides a first estimate of the two components, endowed with an optimisation method devoted to the improvement of the estimation of such two components, with special attention to the localisation of

the temporal support of the non-propagating component. The results obtained by the adaptive filter method have been compared to those obtained after optimisation. The optimised method gives always an improvement (whose importance depends on the actual signals considered), but requires a higher computational cost.

The method was applied to separate non-propagating components in surface EMG signals detected by three channels along muscle fibres. It was first optimised on simulated test signals. Then the performance of the method was tested on phenomenological and simulated signals, before applying it to some representative examples of experimental signals. A first example of application was the identification of the propagating and non-propagating components in single MUAPs detected by a linear array of three electrodes. A second application was the removal of the stimulation artifact from M-waves recorded with three single differential channels during transcutaneous electrical stimulation. The method proposed in this paper is robust to noise and shape perturbations of the two components in simulated signals (improving substantially the results shown in [13]). This suggests that the method can be applied (even if the hypothesis of the method are not exactly satisfied) on real single MUAP and M-waves. Furthermore, it applies also in the case of non propagating component being identical in all channels (such case can not be studied by the method in [12]).

The method can only be applied to signals that (within a good approximation) are constituted by a single propagating component and a single non-propagating one. For example, interference surface EMG signal cannot be processed by the method. Also single MUAPs are not exactly feasible, as the amplitudes of the generation effect across different channels decay in the opposite directions with respect to the amplitudes of the end of fibre effect. Nevertheless, the method was applied on simulated SFAPs, and could identify the location of both generation and extinction effects. This is an important improvement with respect to the method proposed in [12] by which only extinction effects can be estimated. The new method was assessed by comparing the estimated propagating and non-propagating components with those obtained directly from the simulated signals. It was verified that the adaptive filter method allows to identify both the generation and the extinction effect. The optimisation method improves the estimation of both the propagating and non-propagating component.

Non-propagating components reflect important properties of the signals under consideration. In the case of single MUAPs, non-propagating components are related to the generation of the action potential at the endplates and its extinction at the tendon endings. The localisation of the non-propagating components in this case gives, for example, information about the location of the endplate and tendons, and therefore on the mean length of the fibres constituting the MU.

The optimisation method, improving the localisation of the non-propagating components, improves also the estimation of the propagating component, which is often superimposed on the non-propagating one.

In conclusion, we proposed a novel approach to identify and separate the propagating and non-propagating components from EMG recordings in which one propagating and one non-propagating component are present. The technique may find different applications. In single MUAP studies, it could be useful to decrease the variability and bias of CV estimates due to the presence of the non-propagating components. It could also be applied to the automatic identification of the positions of the innervation zone and of the tendons. Furthermore, stimulation artifact can be considered as a non-propagating component and removed before processing the M-wave.

REFERENCES

- [1] H. Broman, G. Bilotto, C. De Luca, "A note on non invasive estimation of muscle fiber conduction velocity", *IEEE Trans. Biomed. Eng.*, 32, pp. 341-343, 1985.
- [2] N.A. Dimitrova, G.V. Dimitrov and Z.C. Lateva., "Influence of the fiber length on the power spectra of single muscle fiber extracellular potentials", *Electromyogr. Clin. Neurophysiol.*, 31(6), pp. 387-398, 1991.
- [3] D. Farina and R. Merletti, "Methods for estimating muscle fiber conduction velocity from surface electromyographic signals", *Medical & Biological Eng. & Computing*, 42(3), pp. 432-445, 2004.
- [4] L. Mesin, M. Joubert, T. Hanekom, R. Merletti, D. Farina, "A Finite Element Model for Describing the Effect of Muscle Shortening on Surface EMG", *IEEE Trans. Biomed. Eng.*, 53(4), pp. 593-600, 2006.

- [5] E. Schulte, D. Farina, R. Merletti, G. Rau, C. Disselhorst-Klug, "Influence of muscle fibre shortening on estimates of conduction velocity and spectral frequencies from surface electromyographic signals", *Medical & Biological Eng. & Computing*, 42(3), pp. 477-486, 2004.
- [6] L. Arendt-Nielsen and M. Zwarts, "Measurement of muscle fiber conduction velocity in humans: techniques and applications", *J. Clin. Neurophysiol.*, 6, pp. 173-190, 1989.
- [7] D. Farina and R. Merletti, "A novel approach for precise simulation of the EMG signal detected by surface electrodes", *IEEE Trans. Biomed. Eng.*, 48, pp. 637-646, 2001.
- [8] Z. Cheng and T. T. Tjhung, "A new time delay estimator based on ETDE," *IEEE Trans. Signal Processing*, 51, pp. 1859-1869, 2003.
- [9] D. Farina, L. Mesin, S. Martina and R. Merletti, "Comparison of spatial filter selectivity in surface myoelectric signal detection: influence of the volume conductor model", *Medical & Biological Eng. & Computing.*, 42(1), pp 114-120, 2004.
- [10] E. Schulte, D. Farina, G. Rau, R. Merletti and C. Disselhorst-Klug, "Single motor unit analysis from spatially filtered surface electromyogram signals. Part 2: conduction velocity estimation", *Medical & Biological Eng. & Computing*, 41(3), pp 338-345, 2003.
- [11] D. Farina and R. Merletti., "A novel approach for estimating muscle fiber conduction velocity by spatial and temporal filtering of surface EMG signals", *IEEE Trans. Biomed. Eng.*, 50, pp. 1340-1351, 2003.
- [12] L. Mesin, F. Tizzani, D. Farina, "Estimation of Muscle Fiber Conduction Velocity from Surface EMG Recordings by Optimal Spatial Filtering", *IEEE Trans. Biomed. Eng.*, 53, pp. 1963-1971 2006.
- [13] J. Rubio Vela, R. Merletti and Y. Fan, "Separation of travelling from non-travelling components in surface myoelectric signals". Proceedings of the VI Mediterranean Conference on Medical and Biological Engineering. vol. I. July 5-10, 1992 Capri, Italy.
- [14] F. Mandrile, D. Farina, M. Pozzo, R. Merletti, "Stimulation artifact in surface EMG signal: effect of the stimulation waveform, detection system, and current amplitude using hybrid stimulation technique", *IEEE Trans. Neural Syst. Rehabil. Eng.*, 11(3), pp. 407-415, 2003.
- [15] F. Mandrile, F. Assumma, D. Farina, K. Englehart, P.A. Parker, R. Merletti, "A Novel Adaptive Filtering Approach for Removing Stimulation Artifact from M-waves", Proc. XV Congress of the

International Society of Electrophysiology and Kinesiology, Boston, MA, June 18-21, 2004, ISBN 0-87270-136-0, p. 77.

[16] J. Rubio Vela, "Characterization and separation of propagating and stationary myoelectric signals", Master Thesis, Boston University, 1990.

[17] Y.X. Tu, A. Wernsdorfer, S. Honda, Y. Tomita, "Estimation of conduction velocity distribution by regularized-least-squares method", *IEEE Trans. Biomed. Eng.*, 44(11), pp. 1102-1106, 1997.

[18] D. Farina, L. Mesin and S. Martina, "A Surface EMG generation model with multilayer cylindrical description of the volume conductor", *IEEE Trans. Biomed. Eng.*, 51(3), pp. 415-426, 2004.

[19] M. Gazzoni, D. Farina, R. Merletti, "A new method for the extraction and classification of single motor unit action potentials from surface EMG signals", *J. Neurosci. Methods*, 136, pp.165-177, 2004.

[20] C. Disselhorst-Klug, G. Rau, A. Schmeer, J. Silny, "Non-invasive detection of the single motor unit action potential by averaging the spatial potential distribution triggered on a spatially filtered motor unit action potential", *J. Electromyogr. Kinesiol.*, 9, pp. 67-72, 1999.

FIGURE CAPTIONS

Figure 1. Block diagram of the proposed optimisation process. a) Adaptive filter algorithm proposed in [13] for a selected τ value. b) Optimisation algorithm proposed in this work.

Figure 2. Interpolation process applied to a simulated single fibre action potential (simulation parameters: fibre symmetric with respect to the innervation point; semi-length of the fibre 80 mm; depth of the fibre 5 mm; transversal distance of the fibre with respect to the detection array 0 mm; angle of inclination of the fibre with respect to the detection system 0° ; sampling frequency 2048 Hz; conduction velocity 4 m/s; interelectrode distance 5 mm). Four time instants are defined, a): t_1 and t_2 define the time interval considered for generation; t_3 and t_4 define the time interval considered for extinction. The propagating component in the generation and extinction time interval was estimated using a 4th order polynomial fitting, considering 8 samples for each time interval: 3 samples before and 5 samples after generation for the estimate in the generation time interval; 5 samples before and 3 samples after extinction for the estimate in the extinction time interval. The application of the method on three channels is shown in b). The three input signals are shown in b1). Three propagating signals have been estimated as described in a), they were aligned and averaged to obtain the estimated averaged propagating signal shown in b2). The non-propagating components, b3), were estimated by subtracting the estimated averaged propagating signal (properly delayed and weighted) from the input signals in b1). A.U. means arbitrary units.

Figure 3. Representative example of choice of the penalisation parameter (same simulated signals as shown in Figure 2). The penalisation parameter γ was varied in discrete steps of 0.1 each, starting from zero. By increasing the regularisation parameter, the reconstruction errors of the two components decrease, they attain a minimum (for $\gamma \cong 0.4$), and then increase again (propagating component, a); non-propagating component, b)). The reconstruction error of the data, c), and the energy of the reconstructed non propagating component (which is the regularisation function), d), have a sigmoid shape as a function of the regularisation parameter. In correspondence of the minimum errors in the reconstruction of the propagating and non-propagating components (unknown for real signals), the reconstruction error of the data and the energy of the reconstructed non

propagating component (which can be calculated also on experimental signals) undergo an abrupt change. The value corresponding to such change is selected as γ_{opt} .

Figure 4. Estimated propagating and non propagating components estimated using the adaptive filter method and the optimisation method when some of the hypothesis of the model (Section 2.A) are not

met: a), b) example with phenomenological signals (coefficient matrix $\underline{\underline{A}} = \begin{bmatrix} 1 & 1 \\ 0.9 & 0.8 \\ 0.85 & 0.75 \end{bmatrix}$, delay

$\tau=1.25$ ms, sampling frequency 2048Hz), where the width a) and the delay b) of the propagating component in the second channel is perturbed by +5% and +15%, respectively, with respect to the other channels. The propagating and non propagating component estimated using adaptive filter technique and optimisation method match well with the original simulated components (without perturbation). To quantify the correctness of the reconstruction, the RMS error (normalised with respect to the square root of the average energy of the three input measures) between the non-propagating component estimated by the separation method and the true one is shown in c) and d). Both percent RMS errors in estimating the non propagating component for percentage variation between -15% and 15% of the delay, c), and for width changes in the second channel between -10% and 10%, d), are shown. Ten realisations of Gaussian white noise were considered at 20dB SNR for each case.

Figure 5. Example of separation of propagating and non-propagating component in a simulated signal, a) (same simulated signal as in Figure 2). Reconstruction of the non-propagating signals by adaptive filter, b), and after optimisation, c), and comparison with the reference ones obtained by the interpolation method (see Figure 2). The estimated non-propagating signals obtained by the adaptive filter method and the optimised one are shown in d). Travelling signals estimated by adaptive filter, e), and after optimisation, f), and comparison with the average of the three propagating components obtained by the interpolation method and used as reference (see Figure 2).

Figure 6. Comparison between separation methods applied to simulated signals (plane layer surface EMG generation model [7]) related to different simulated anatomies. List of model default parameters: cylindrical model with four layers (bone, 20 mm radius, conductivity 0.02 S/m; muscle,

thickness 26 mm, longitudinal conductivity 0.5 S/m, transversal conductivity 0.1 S/m; fat, thickness 3 mm, conductivity 0.05 S/m; skin, thickness 1 mm, conductivity 0.5 S/m), depth of the fibre within the muscle 5 mm, semi-length of the fibre 70 mm, angle of inclination with respect to the detection array 0° , transversal distance with respect to the detection array 0 mm. a) Variation of depth of the fibre within the muscle (2 mm to 10 mm in discrete steps of 2 mm). b) Variation of semi-length of the fibre (60 mm to 80 mm in steps of 5 mm). c) Variation of transversal distance with respect to the detection array (0 mm to 8 mm in steps of 2 mm). d) Variation of the angle of inclination of the fibre with respect to the detection array (0 to 15 degrees in steps of 3 degrees). To quantify the correctness of the reconstruction, the following RMS errors were studied: the RMS error between the propagating component estimated by the separation method and the propagating component estimated by interpolation on the simulated signals (see Figure 2); the RMS error between the non-propagating component estimated by the separation method and the non-propagating component estimated by interpolation on the simulated signals. Ten realisations of additive noise were considered (Signal to Noise Ratio, SNR, 20dB).

Figure 7. Application of the adaptive filter and optimised methods to the estimation of fibre semi-length. Single fibre action potentials were simulated (same generation model as in Figure 6), in order to have a defined fibre length. The method to estimate the delay between the generation and extinction effects is explained in a). The percentage error of the estimation with respect to the simulated length of the fibre as a function of such length is shown in b), c), d) for fibres which are superficial (3 mm depth), deep (6 mm depth) and transversally displaced with respect to the detection array (5 mm transversal distance), respectively. Ten realisations of additive noise were considered for each simulation (Signal to Noise Ratio, SNR, 20dB).

Figure 8. Example of application to three channels of monopolar surface EMG signals, a), b), c), collected from the abductor pollicis brevis muscle (linear array of 3 electrodes, placed along the direction of the muscle fibres, with inter-electrode distance 5 mm). Contractions 60 s long at force lower than 4 % of the maximal voluntary contraction force were decomposed. One spike-triggered averaged single MUAP is considered. The monopolar signals were normalised with respect to the negative peak value in order to compensate for possible large variations in the amplitude of the

propagating component across the channels. The propagating, b), and non-propagating, c), components estimated by adaptive filter and optimised method are shown. Example of a surface EMG signal recorded during transcutaneous electrical stimulation of the biceps brachii muscle, d), e), f). The propagating (M-wave), e), and non-propagating (artifact), f), components estimated by adaptive filter and optimised method are shown.

Fig 1

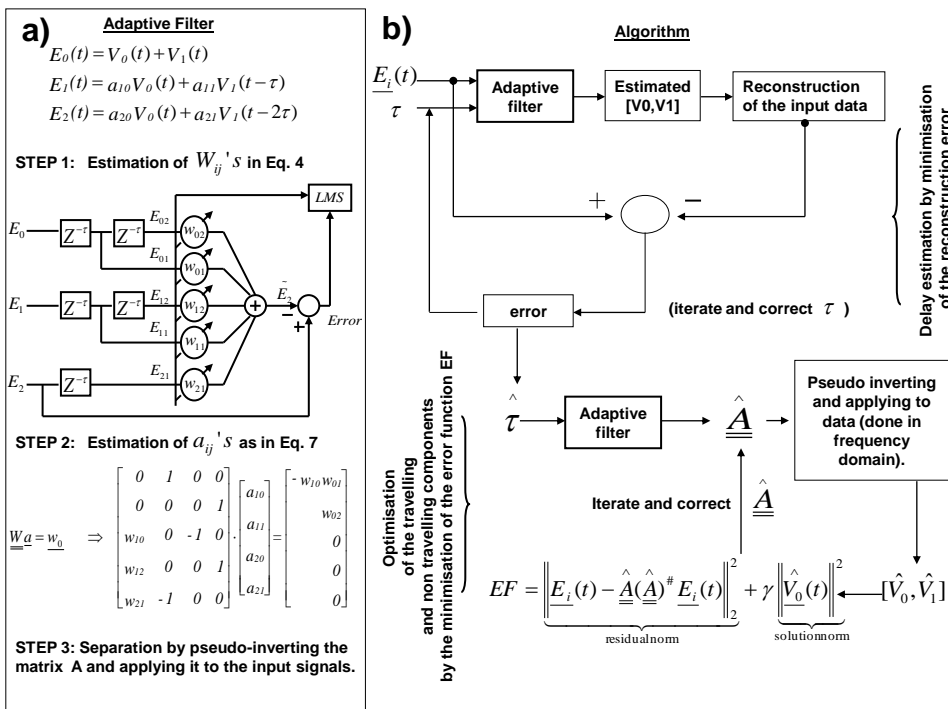


Fig 2

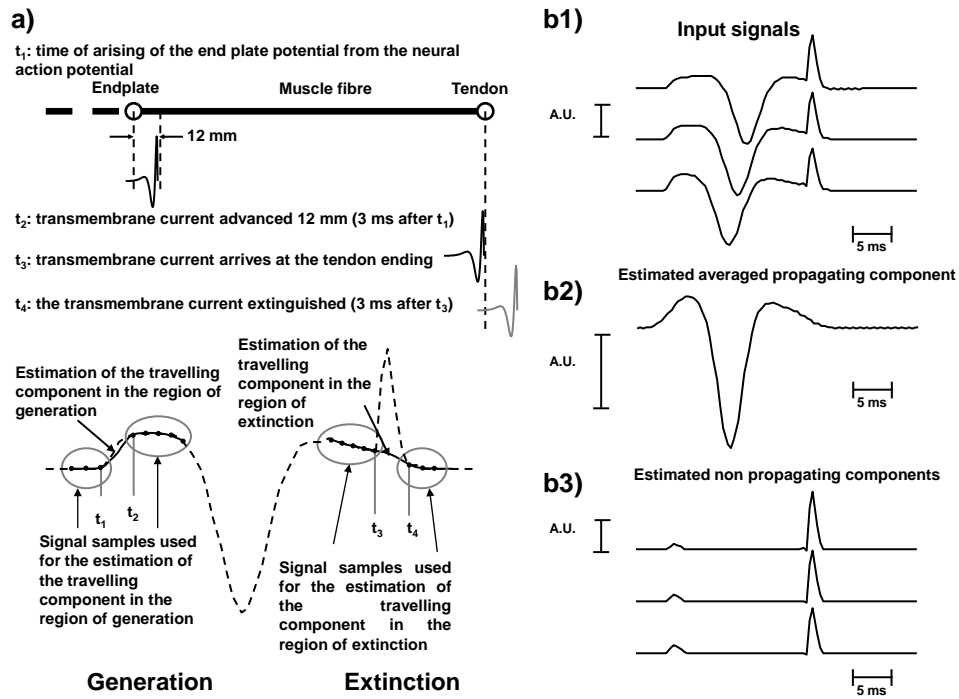


Fig 3

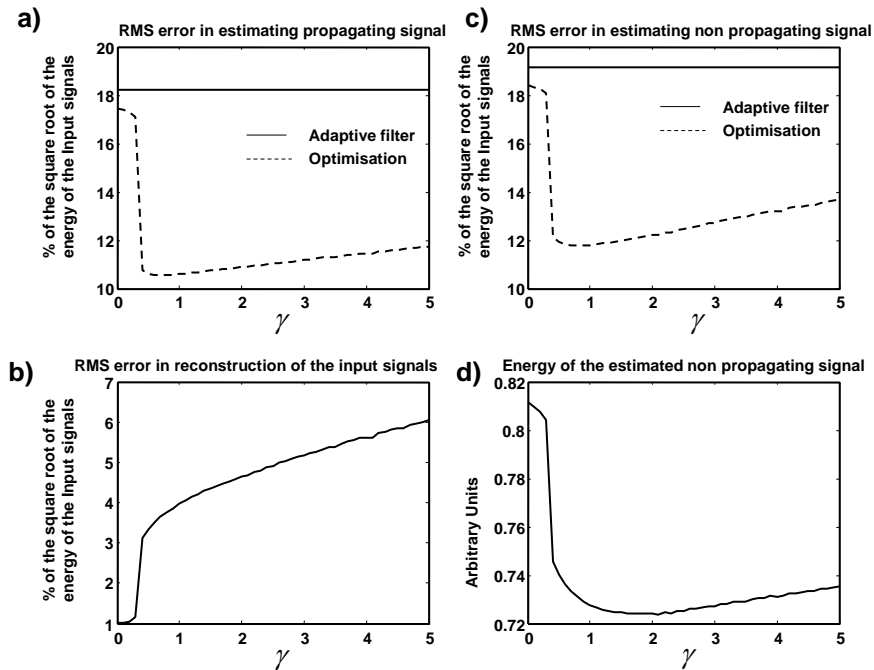


Fig 4

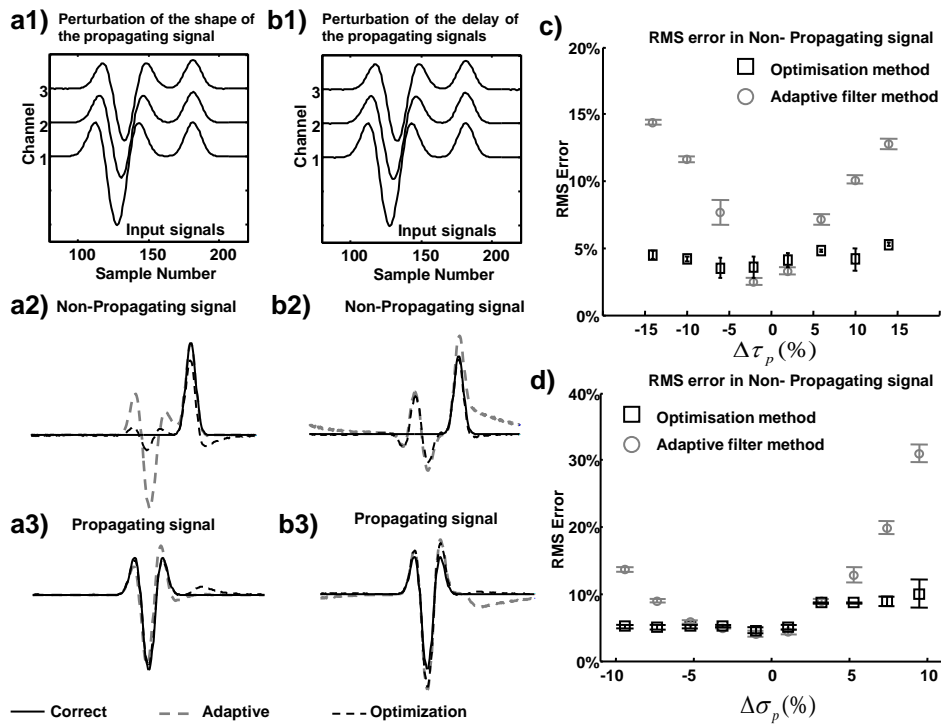


Fig 5

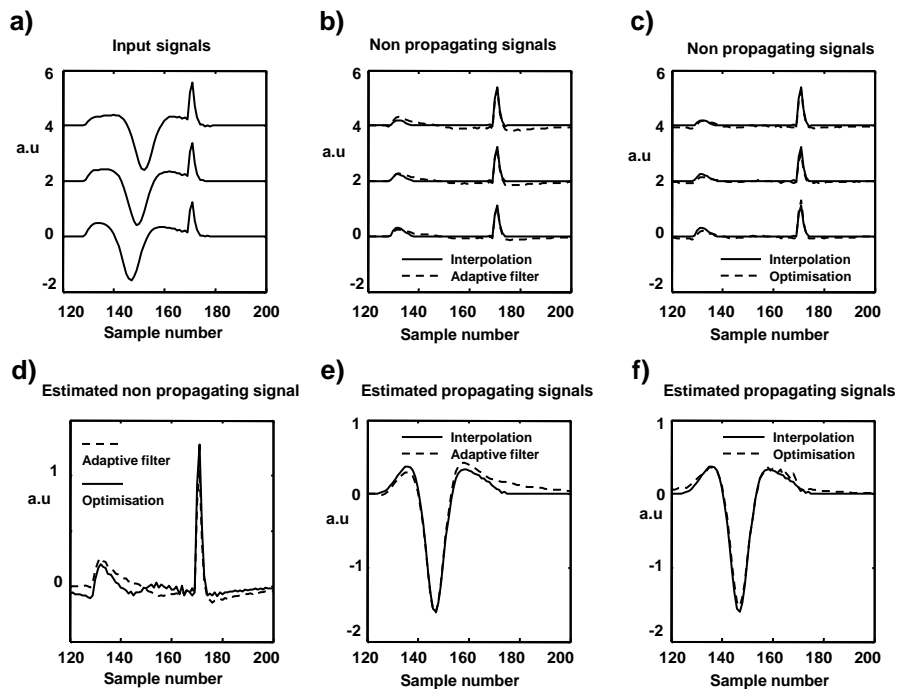


Fig 6

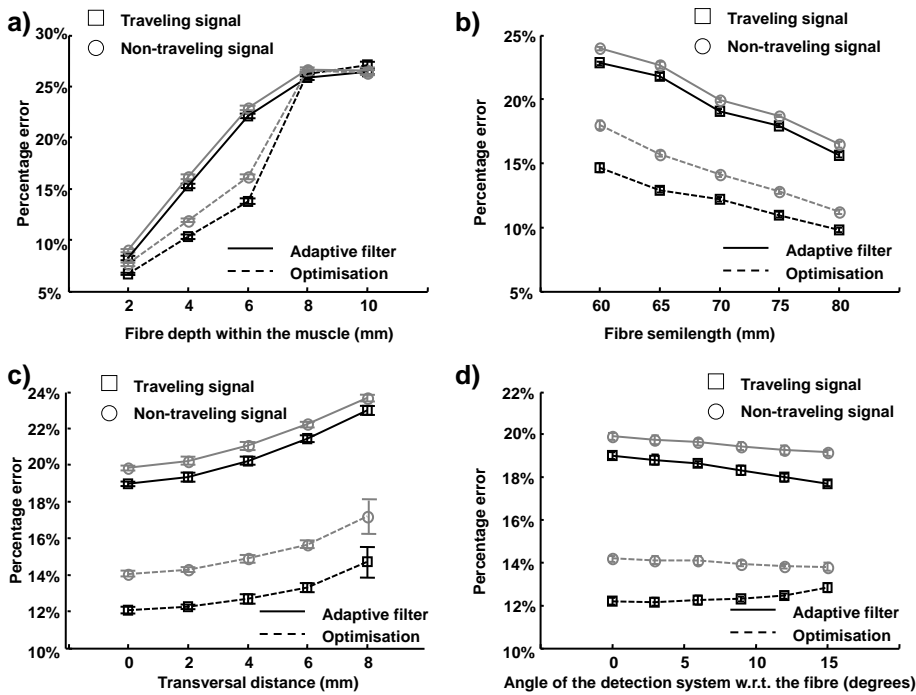


Fig 7

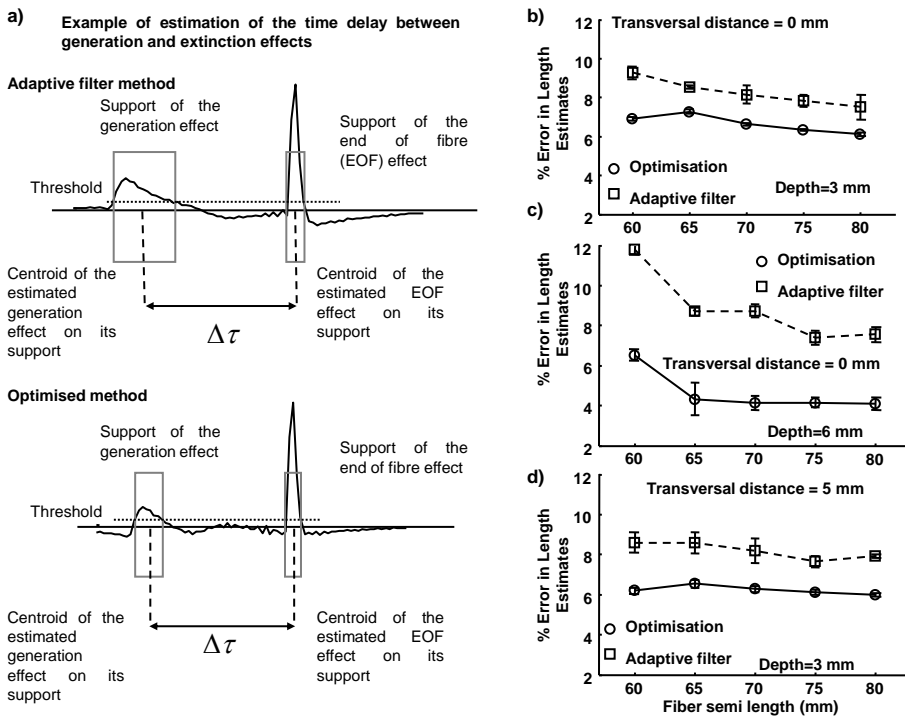


Fig 8

